J. Min. Metall. Sect. B-Metall. 54 (1) B (2018) 39 - 50

Journal of Mining and Metallurgy, Section B: Metallurgy

EXPERIMENTAL CARBOTHERMAL REDUCTION OF MgO AT LOW PRESSURE USING CONCENTRATED SOLAR ENERGY

J. Puig *, M. Balat-Pichelin

PROMES-CNRS Laboratory, Font-Romeu, France

(Received 15 February 2017; accepted 02 October 2017)

Abstract

The improved solar reactor Sol@rmet allows to investigate the reduction of MgO in presence of carbon using concentrated solar energy in low vacuum conditions close to 900 Pa. The influence of the carbon type was studied and it was shown that a carbon issued from a biomass source was a great candidate. A gradual increase of the temperature during experiment allowed to obtain promising results. Powders with a high Mg content up to 97 m% and a high yield rate up to 50% were collected. Short time experiments at fixed locations under the focus of the solar concentrator were performed in order to obtain information on the kinetics of the carbothermal reduction of MgO. Notably, these experiments have underlined the temperature effect on the CO emission. 50 to 80% of the CO emission mainly occurred in 100 s after the beginning of the experiments. The phase boundary reaction between MgO and C appeared to be the dominant process at the initial stage of the carbothermal reduction. Calculated activation energy of this process is around 260 kJ mol^{-1}.

Keywords: *Carbothermal reduction; Concentrated solar energy; XRD characterization; Microstructure; Kinetics*

1. Introduction

The use of solar energy for the production of metals from their oxides with a carbothermal process was considered since the 90's in order to promote renewable energy and to reduce the greenhouse gases in the extractive metallurgical industry [1-7]. Notably, it had been proved that ZnO is decomposed into Zn using high-temperature solar processes and successful solar carbothermal reduction of ZnO was developed with a solar pilot of 300 kW [1-4, 7].

In order to build a sustainable development, the use of new energetic, clean and recyclable fuels will be necessary. In particular, in the transportation field, the current used fossil fuels have limited resources and reject a great amount of greenhouse gases. One of the most interesting proposed alternatives concerned the direct combustion of recyclable metal fuels [8]. As an example, aluminum (Al) has already extensively been used as propellant in rockets and recent studies have been done in order to accurately evaluate the combustion regime of micron-sized aluminum powders for fuel applications [9]. Magnesium (Mg) is also a very attractive potential fuel due to its high energy density close or larger than the ones of fossil fuels. The thermal reduction of magnesium compounds was already studied since the 40's [10]. However, the recycling of Mg from MgO remains a problem for the global warming as high carbon sources are used for the high energy input of the main process (Pidgeon) although some recent improvements have been realized [11, 12]. In order to reduce greenhouse gases emissions, a great part of the energy input for this reaction could be provided by concentrated solar energy that is an accessible, inexhaustible and clean energy source, and that allows reaching high temperatures in short times. The use of a reducing agent allows a decrease of the reduction temperature of MgO due to the lower energy needed for the carbothermal reaction than the one required for the thermal decomposition of MgO and to an increase of the solar absorptivity of the MgO mixture. It had been calculated that it is possible to reduce MgO at 2130 K at atmospheric pressure ($\Delta G_{2130\,K,\,105\,Pa} = 0$) [5, 6]. At 2000 K, the overall reaction can be represented by:

$$MgO_{(s)} + C_{(s)} = Mg_{(g)} + CO_{(g)}$$
$$\Delta G_{2000\,K,\,105\,Pa} = 34.0 \text{ kJ mol}^{-1} \quad [13] \quad (1)$$

Under vacuum, the temperature of the carbothermal reduction of MgO is theoretically lowered, which had been demonstrated by thermodynamic calculations assuming closed systems and indicating that MgO could be reduced with carbon at 1360-1400 K at 10 Pa [14-15]. Notably, the reduction temperature appeared to be more important when the pressure goes down from 10^5 Pa to 10^2-10^3 Pa [15].

*Corresponding author: jean.puig@promes.cnrs.fr

DOI:10.2298/JMMB170215048P

Recent feasibility of solar carbothermal reduction of MgO under vacuum has been demonstrated using a direct irradiation of the pellet or in a cavity [15, 16]. Powders with high metallic content were obtained but Mg yields of 45 and 62 % were reached due to the formation of MgO in the collected powders and to the sintering of MgO particles in the reactants [16].

The reaction mechanisms and kinetics of the carbothermal reduction of MgO were well described by a phase boundary reaction based on reaction (1) [17]. The grade of the carbon source appeared to have an influence on the reaction mechanism. As an example, Galvez et al. obtained higher metallic yields with petroleum coke (85.4 % of Mg) than with wood charcoal after 200 minutes at 1823 K. The reaction with this reducing agent could be better described by a solid-gas kinetic model, which could demonstrate a more important role of the CO diffusion at high temperatures through the following relation [18]:

$$MgO_{(s)} + CO_{(g)} = Mg_{(g)} + CO_{2(g)}$$
$$\Delta G_{2000\ K,\ 105\ Pa} = 209.7\ kJ\ mol^{-1} \quad [13] \quad (2)$$

At high temperatures, carbon dioxide directly reacts with carbon following the Boudouard reaction:

$$C_{(s)} + CO_{2(g)} = 2\ CO_{(g)}$$
$$\Delta G_{2000\ K,\ 105\ Pa} = -175.7\ kJ\ mol^{-1} \quad [13] \quad (3)$$

Rongti et al. described two different stages for the carbothermal reduction of MgO with reaction at the interface between MgO and C grains (Eq. (1)) as the initial stage below 1750 K and a more important role of CO diffusion (Eq. (2)) during the last stage above 1750 K [19]. Recently, Xie et al. have studied the kinetics of the carbothermal reduction of dolomite (ore with a high Mg content) at 10 Pa and 1573 K and they have calculated activation energies of 220 kJ mol^{-1} for a phase boundary reaction (close to 208 kJ mol^{-1} calculated by Rongti et al. and 222 kJ mol^{-1} by Prentice et al. [17, 19]) and of 451 and 529 kJ mol^{-1} for gaseous diffusion phenomena (373 kJ mol^{-1} for Rongti et al [19]) [20]. Fruehan et al. have demonstrated that the reaction primarily occurred at the interface but suggested that the overall rate was controlled by the gaseous diffusion through a porous MgO layer that could be formed on the sample surface [21]. A model has been recently developed showing that the solid-solid reaction is the main mechanism controlling the first stage of the reaction whereas gas-solid reactions could allow to complete the carbothermal reduction of MgO depending on the system pressure [22].

Another major problem of the carbothermal reduction of MgO concerns the reversion reaction between CO and produced Mg. Shafirovich and Goldshleger proved that the reverse reaction of Eq. (1) is kinetically slow which indicates that condensed Mg has to be formed before reversion can proceed [23]. Two carbothermal reduction routes were described to prevent this reaction: rapid quenching of the vapors or dissolving the magnesium directly in a suitable metal solvent [24]. Engell et al. used a rapid quenching of the Mg vapors in a condensation zone cooled below 800 K at 10-10^4 Pa but there is no published data on this patented work [25]. The Magsonic™ process used a Laval nozzle at temperature above 1970 K and at atmospheric pressure with reversion below 10%, which demonstrated the possibility to obtain high Mg yields [26]. Finally, it had been recently demonstrated that rapid oxidation of $Mg_{(g)}$ occurred in the presence of CO_2 and that it is necessary to have low CO and CO_2 partial pressures to obtain high metal yield [27] .

In this study, an improved solar reactor Sol@rmet was designed in order to optimize the carbothermal reduction of MgO using concentrated solar energy and a primary vacuum of 900 Pa following our previous work using another reactor Heliotron [15]. A 2 kW solar furnace facility was used to concentrate solar energy. The first part of this work is dedicated to the production of nearly pure Mg powders with high yield rate through experiments using various carbon grades and heat treatments. In a second part, the effect of the temperature on the CO emission is underlined. For the first time concerning the carbothermal reduction of MgO using concentrated solar energy, these emissions are correlated to kinetics equations in order to determine the main process at the initial stage. The role of the different processes are finally discussed and compared with literature data.

2. Experimental

2.1. Preparation of the reactants

Mixtures of MgO (Sigma Aldrich, 325 mesh, > 99 %) with carbon black (Cabot Carbone, 38-40 $m^2\ g^{-1}$, carbon content > 99%) or with a biochar (Carbon Terra, birch tree pyrolyzed at 770 K, 4 h, Ø < 12 μm, carbon content > 94 %) as a source of reducing agents were prepared using the following molar ratios MgO:C = 1:1.5 or 1:1.25. An excess of carbon was used due to primary investigations indicating that the reaction was more complete with a greater amount of carbon close to 1.25-1.5 moles than using a stoichiometric mixing [15]. Powder mixtures were pressed at 1 ton to form pellets (Ø 8 mm, thickness from 1 to 2.5 mm). For each experiment, one pellet was placed on a graphite cylinder (resisting to high heating rates and with a reasonable thermal conductivity) positioned on the water-cooled sample-holder.

2.2. Design of the solar reactor and experimental conditions

A solar reactor called Sol@rmet was built to study the carbothermal reduction of metallic oxides in low vacuum at high temperature. A schematic layout of this reactor and set-up is presented in Fig. 1a. Sol@rmet (Fig. 1b) is divided into 2 parts: a transparent glass dome for the entry of the concentrated solar radiation constitutes the upper zone; the lower section is made with a cooled double wall in stainless steel in order to resist to high temperatures.

A 2 kW solar furnace facility located in Odeillo, France, able to concentrate solar energy up to 11 000 suns (1 sun ≈ 1000 W m^{-2}), was used for the experiments. The heliostat, equipped with a sun tracking system, vertically reflects the direct solar flux on a stationary parabolic mirror. Solar energy is concentrated in a focal zone. An adjustable shutter placed in between the heliostat and the parabolic mirror allows controlling the incident solar flux on the pellet and thus its temperature.

The direct normal irradiance (DNI) was nearly constant during the experiments presented in this study, and was in the range 975-1040 W m^{-2}. A dry primary pump allowed to reach a constant pressure of 900 Pa with flowing argon (5 Nl min^{-1}). Argon was injected in the upper part of the glass dome in order to avoid deposits on the fluorine window used for temperature measurement by optical pyrometry. An oxygen content lower than 5 ppm was measured in the reactor, which limited oxidation of the metallic vapors. Metallic vapors mainly condensed on a ZrO_2-TiO_2 filter (0.1-0.2 µm) positioned just before a primary vacuum pump, as shown in Fig. 1. Some little amount of products was also present on the metallic lower section of the reactor and on the sample-holder but it represents less than 10 m% of the deposits.

The temperature of the sample surface was measured using a pyrometer Heitronics K15.42 (wavelength 4.9 - 5.5 µm) positioned above the Sol@rmet reactor. A normal spectral emissivity of 0.95 of the mixtures MgO/C was taken for temperature measurements by monochromatic pyrometry considering reflectivity measurements carried out at ambient temperature at PROMES-CNRS laboratory and previous results issued from literature obtained at higher temperatures [28]. The solar flux distribution close to the focus is represented by a Gaussian curve, as presented in Fig. 2a but the optical pyrometer indicated the mean temperature on all the surface sample (8 mm diameter). However, preliminary modeling results (Fig. 2b) indicated that the measured temperature by optical pyrometry is by around 100 to 200 K higher than the mean temperature on the whole surface of the sample. So, the mean temperature on the whole surface of the sample could be lower than those indicated by the pyrometer. CO and CO_2 emissions were monitored during experiment using an infrared gas analyzer X-Stream X2GP to follow the reaction kinetics. The time response of the analyzer appeared to be lower than 2s.

This reactor has three advantages than the previous one already used [15]:

- the volume of the reactor is smaller (2 L vs 6 L), which limits the deposit zones,
- it is possible to measure the temperature during the experiment by optical pyrometry and an analysis of the gas emitted is recorded,
- the air-tightness has been improved, which limits the possible reversion reaction between Mg produced and O_2 from the air.

Two different procedures were used for the solar experiments:

a) Experiments in order to obtain high yield rates: the samples were placed on the graphite sample-

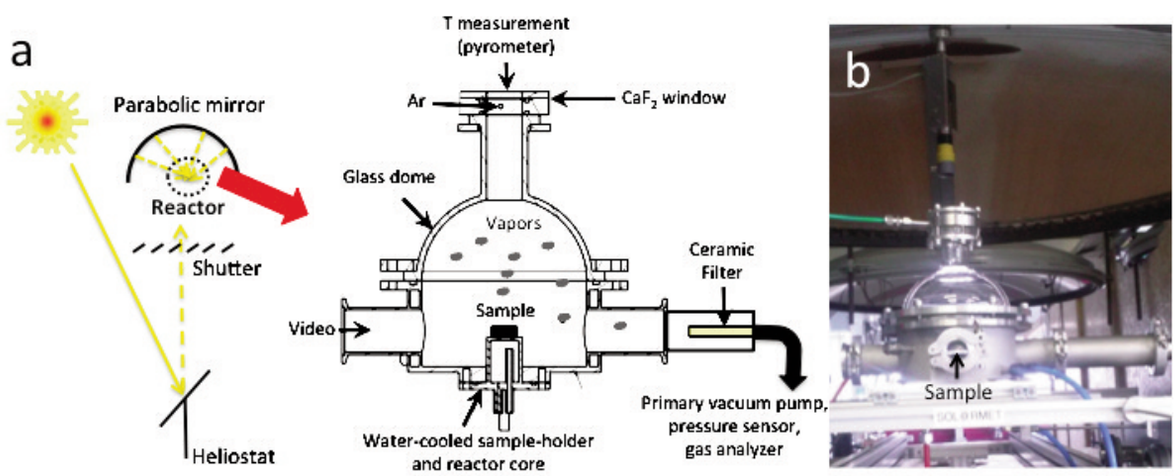

Figure 1. *a) Schematic layout of the solar reactor experimental set-up used at PROMES-CNRS laboratory, b) Sol@rmet at the focus of the parabolic mirror before an experiment*

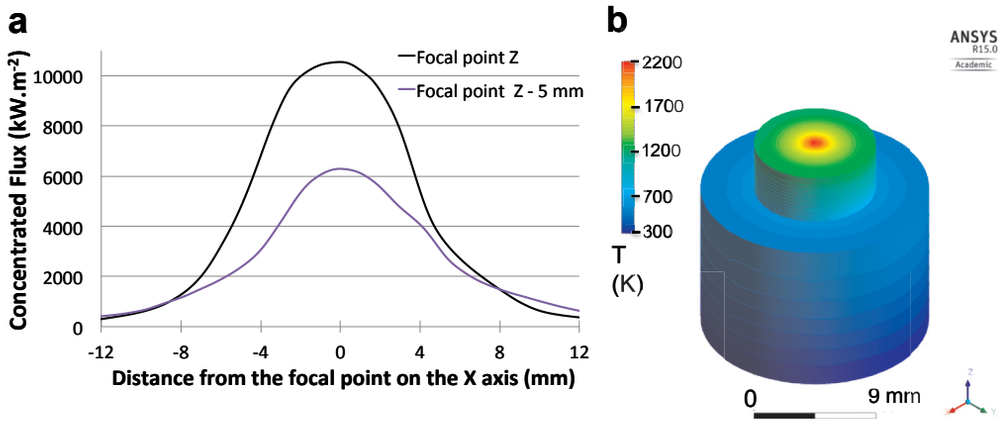

Figure 2. *a) Flux distributions of the concentrated solar energy at the focal point (X,Y,Z) and 5 mm below this point, b) Modeling result showing the thermal gradient on the pellet surface during a solar experiment (scale at the bottom)*

holder and were gradually raised from 25 mm up to a minimum of 9 mm below the focal zone with the shutter fully open. The reaction temperature increases when the sample is moving closer to the focal zone of the parabolic mirror. Different durations were used between the raising steps at different sample positions.

b) Experiments for kinetic calculations at fixed temperature: the samples were positioned at a fixed distance (from 10 to 4 mm) below the focal zone during 620 s and the shutter was opened at 65-70 %. CO and CO_2 emissions and temperature were monitored in order to evaluate the critical limiting rate process. In order to avoid an important temperature gradient in the sample (which could be detrimental for kinetics calculations purpose), only 61-63 mg of mixed powders have been pressed into a pellet for these experiments. The temperature of the sample surface was supposed to be reached 15 s after the beginning of the experiments, the shutter being open in 10 s. However, the measured temperature by optical pyrometry was stable only 25 s after the beginning of the experiments due to a great emission of vapors disturbing the measurement during few seconds. Considering this fact, we assumed that we had quasi-isothermal conditions 15 s after the beginning of the recorded experiments when the CO emission began. So, making the approximation of isothermal conditions 15 s after the beginning of the experiment, it appeared possible to make kinetic calculations.

2.3. Characterization of the collected powders

After each solar experiment, powders deposited on the ceramic filter and on the metallic walls were collected and weighted using a precision balance Sartorius 2462 with a resolution of 0.1 mg.

An X-ray diffractometer X PANalytical X'Pert PRO (θ-2θ) was used to obtain structural information and the chemical composition of the collected powders. Quantitative phase analysis was performed with the Highscore Plus software. This software allows to compare the quality of the collected powders after the solar experiments using the reference intensity ratio technique with the files from the International Centre for Diffraction Data [29, 30]. The accuracy of the analyses depends on various parameters (sample morphology, software accuracy). Taking into account the mass and the quantitative phase analysis of the collected powders, a Mg yield was calculated for each experiment using the expression:

$$Mg\ yield(\%) = ((m_{filter} + m_{wall})\%Mg_{filter})/m_{max.metal} \quad (4)$$

$$\text{with } m_{max.metal} = m(MgO)_{t=0}\, M(Mg) / M(MgO) \quad (5)$$

where $m(MgO)_{t=0}$ is the initial oxide mass, m_{filter} and m_{wall} are the masses of the powders respectively collected on the filter and on the metallic walls of the reactor and $\%Mg_{filter}$ corresponds to the Mg content of the collected powders on the filter calculated using XRD quantitative phase analysis (Mg content of the powder collected on the metallic wall was close to $\%Mg_{filter}$). At least 99% of the powder deposited on the ceramic filter and around 90% of the powder deposited on the metallic walls were collected after the experiments. The powder deposited on the glass dome was negligeable (max 0.5 mg). Considering these facts, the accuracy on the final yield of the experiment was affected by less than 5%. The accuracy of the XRD to quantify the Mg content was estimated to be close to 10% but it could be higher at Mg content lower than 90 m%.

The ratio $n(CO)_{tot}/n(MgO)_i$ represents the reaction extent based on the total CO emitted ($n(CO)_{tot}$) and on the initial amount of MgO $n(MgO)_i$.

Microstructure observations of the collected powders were performed using a Hitachi S4500 SEM. EDX local analyses (Si (Li) detector) were also

realized to confirm the chemical composition of the obtained powders. Considering the results obtained from EDX local analyses and XRD quantitative analyses, a relative error of ± 10 % was taken into account for the calculations issued from XRD quantitative analyses.

The presence of MgO in the collected powders was due both to recombination reaction (reversion of Eq.1) and to re-oxidation of products during the collection process in air (even if the products were put in a dessicator to avoid oxidation by moisture).

3. Results

3.1. Characterization of the reactants

MgO and carbon powders were observed using SEM. Most of the MgO grains have diameters between few hundred nanometers and few microns. All the MgO grains have a diameter lower than 44 µm and tend to agglomerate (Fig. 3a). The carbon black Cabot Carbone is constituted by agglomerated structured grains (great porosity) with a diameter in the range 10-300 µm (Fig. 3b and 3c). On the other hand, the biochar Carbon Terra contains smaller grains with a medium size around 5 µm and a maximum size under 20 µm (Fig. 3d and 3e). Mixing MgO and carbon powders resulted in a homogeneous distribution of the carbon particles in the MgO matrix (example in Fig. 3f with biochar).

3.2. Effect of carbon variety during a gradually raise of the temperature

The experimental conditions and the results from XRD quantitative analysis of four representative solar experiments of carbothermal reduction of MgO with an excess of carbon (MgO:C = 1:1.5) at 900 Pa are presented in Table 1. X-ray diffraction patterns of the collected powders on the filter after carbothermal reduction of MgO are shown in Fig. 4. When raising the sample closer to the focal point, the first vapors appeared at measured temperatures around 1500-1600 K. Experiment 35 was performed with the carbon issued from a biomass source as reducing agent in between 1580-1700 K, which was close to the temperature of the first vapors. The collected powder contained a high amount of magnesium, which demonstrated that the reaction really began at these temperatures. Nevertheless, only 5 mg had been obtained and the reaction extent is close to 12%.

Using higher temperatures (experiments 33 and 34), a higher mass of powders was collected and a higher Mg content was reached (Table 1 and Fig. 4). Notably, a Mg yield of 50% and a reaction extent of 58% were obtained after experiment 33 where the temperature rose up to 2190 K.

Although a higher Mg content (98%) was reached using similar experimental conditions with carbon black as reducing agent, a lower yield was obtained (experiment 32). Other experiments, not presented here, were also realized with carbon black using different time durations and different progressive heating of the sample but lower yields were also obtained.

The CO and CO_2 partial pressures were respectively lower than 3 and 0.5 Pa during the whole experiments (and respectively lower than 1 and 0.01 Pa after 100 s in each experiment). So, only a little reversion of Eq. 1 could happen at the beginning of the experiments, which can explain the high Mg content of the collected powders. Considering only the consumed mass of reactants (without the residue at the end of experiment), the Mg yield is close to 70% after experiments 32 and 33, which means that

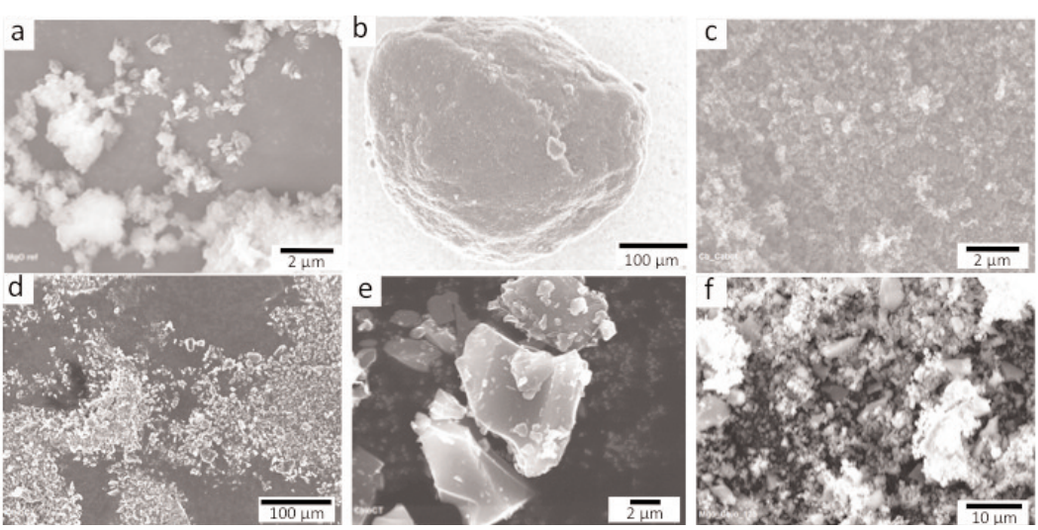

***Figure 3**. SEM images of the reactant powders a) MgO, b) and c) carbon black Cabot Carbone, d) and e) biochar Carbon Terra, and f) mix MgO:C(biochar) = 1:1,25*

Table 1. *Carbothemal reduction of MgO raising the temperature: experimental conditions and results issued from XRD quantitative analysis*

Experiment	Carbon source	Initial mass (mg)	T_{pyro} (K)	$t_{tot.}$ (min)	Collected mass (mg)	$\%Mg_{filter}$ (m%)	Mg Yield (%)	n(CO)t/n(Mg)i (%)
32	Black	145	1700 -> 2190	52	29	98	46 ± 5	51 ± 1
33	Biomass	142	1770 -> 2190	51	31	94	50 ± 7	58 ± 1
34	Biomass	157	1820 -> 1880	40	22	94	32 ± 5	45 ± 1
35	Biomass	121	1580 -> 1700	44	5	85	8 ± 2	12 ± 1

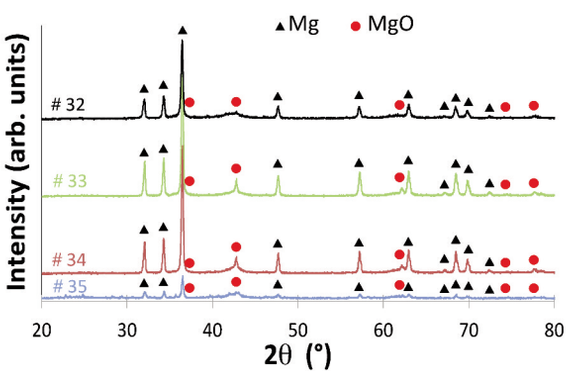

Figure 4*. XRD patterns of the collected powders on the filter after experiments 32, 33, 34 and 35*

30% of the gaseous Mg produced was not recovered into solid Mg essentially due to some losses in the collection process of these low masses. The recombination during the experiments and the oxidation phenomenon during the collection process could not be separated in this study due to the collection of powder in air.

SEM images of the collected powders revealed that the grains diameter was in the range 20-200 µm (Fig. 5a, 5b and 5e). Whatever the carbon source used, the microstructure of the grains was very similar with clusters of agglomerated Mg nanoparticles and Mg crystals with a diameter in the range 2-10 µm (Fig. 5b and 5c). Actually, it has been considered that Mg nanoparticles were formed in the powders due to the fast condensation of gaseous Mg. Considering that MgO is present in the collected powders (XRD analyses), the surface of the nanoparticles/crystals was partially or completely oxidized by residual CO_2(g) (or traces of O_2(g)) to form MgO. Moreover, it had been already proved that CO reacts only with condensed Mg [31]. It is also noticeable that some isolated Mg crystals were present (Fig. 5d and 5f). Nano-sized particles were observed on the surface of the crystals and could be attributed to MgO formed by re-oxidation (Fig. 5d). Residues on the sample-holder at the end of experiments are typically porous (Fig. 6a). SEM images showed some clusters of remaining carbon grains covered by few MgO grains (white grains in Fig. 6a and 6b). It seems difficult to increase the reaction extent over 60-70% due to the presence of around 20-30 m%. of these residues at the end of the

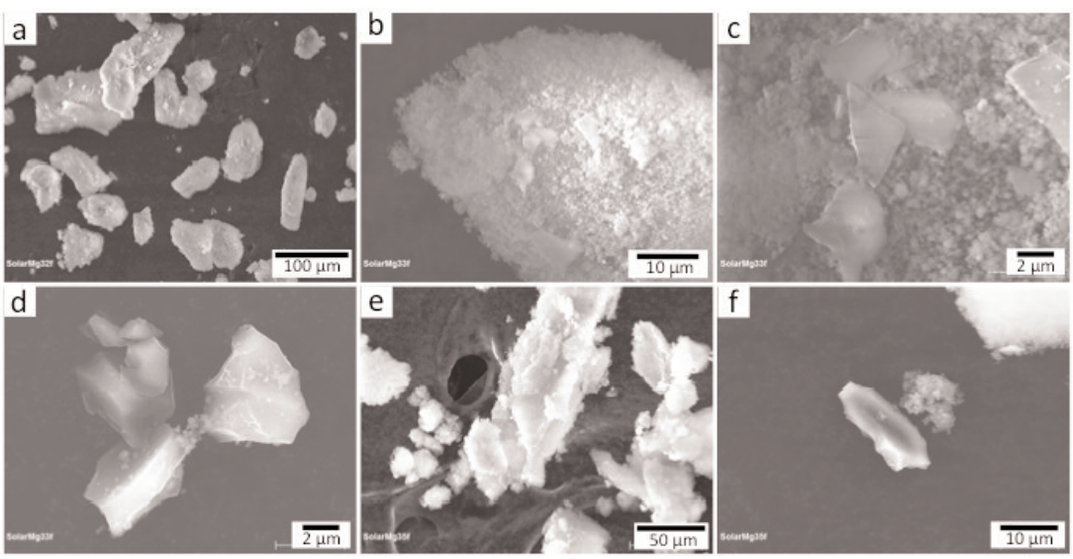

Figure 5*. SEM images of the collected powders on the ceramic filter after experiment a) 32, b), c) and d) 33 and e) and f) 35*

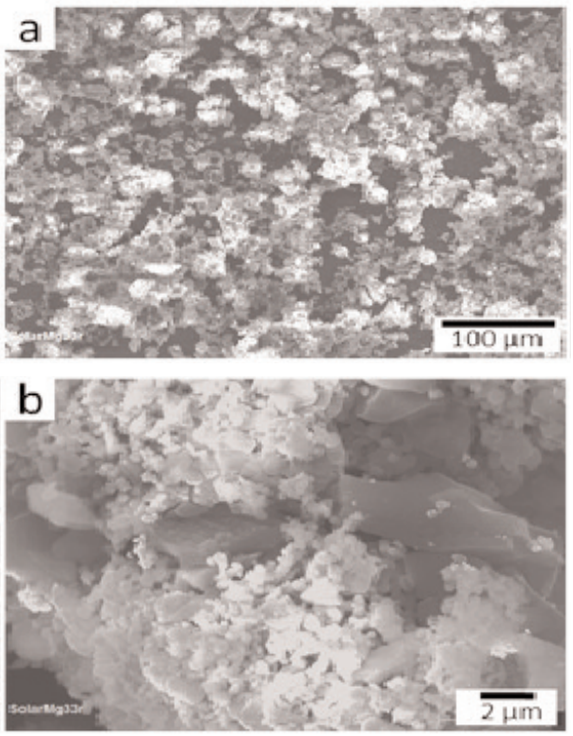

***Figure 6**. SEM images of the remaining powder on the sample-holder after experiment 35*

experiments 32 and 33 (temperature up to 2190 K). The contacts between MgO and C grains must be further optimized in order increase the reaction extent and the reaction could occur faster and/or at a lower temperature.

Considering that better results were obtained with the biochar than with the carbon black and that the biochar could decrease future environmental impacts, this reducing agent was used for the experiments presented in the following section. Furthermore, some experimentations (not presented here) were carried out using a lower excess of carbon (MgO:C = 1:1.25) or a stoechiometric molar ratio between the reactants. These experimentations allowed to obtain maximum similar yields close to 50%, which led to select a lower excess of carbon in the next section in order to decrease the amount of unreacted carbon in the residue.

3.3. Experiments at a fixed temperature using biochar

3.3.1. Effect of the temperature and CO emissions

The experimental conditions and the results from XRD quantitative analysis of four representative solar experiments of carbothermal reduction of MgO at 900 Pa, at fixed temperatures and with a slight excess of carbon (MgO:C = 1:1.25) are presented in Table 2 (*T_{pyro} has been averaged on 20 s after the stabilization of the measured temperature by the optical pyrometer i.e. ~25s after the beginning of the experiment).

Concerning the obtained powders at a hold temperature in the range 2070-2160 K, 7.2 to 8.6 mg was mainly collected on the filter. These powders have a Mg content close to 70-85 m% (MgO was between 15 and 30 m%), which resulted in a total Mg yield close to 20-24%. However, at a higher temperature (2220 K), the collected mass and the Mg content were higher, which resulted in a better Mg yield of 35% (Table 2, experiment n°6). Mg yields are lower than those obtained in section 3.2 because the experimental durations are shorter and due to the fact that the carbothermal reduction of MgO consumes the surface of the sample, which becomes thinner and the temperature decreases at the new surface of the sample which is a little bit more far from the focal zone. If it is considered that the residue does not participate to the reaction, the Mg yield on the reacted mass is close to 40-45% for each experiment. In fact, the loss of products appeared to be more important in these experiments than in the experiments with a gradually raise of the temperature (section 3.2) due to a lower Mg content in the collected powders and to the lower initial mass of reactants, which resulted in lower masses of products more difficult to collect (adherent on the metallic walls and on the filter). The calculated reaction extent based on CO emissions are in a good agreement with the calculated yield using XRD semi-quantitative analysis except for the experiment n°8 (mainly due to more losses in the collection process).

SEM images of the collected powders revealed that grains diameter was in the range 20-200 µm (Fig.

***Table 2.** Carbothermal reduction of MgO at fixed temperatures during 620s: experimental conditions and results issued from XRD quantitative analysis*

Experiment	Initial mass (mg)	T_{pyro}* (K)	Collected mass (mg)	$\%Mg_{filter}$ (m%)	Mg Yield (%)	$n(CO)_{tot}/n(MgO)_i$ (%)
2	62.4	2070	8.6	69	22 ± 2	24 ± 1
3	63.3	2140	8	82	24 ± 2	27 ± 1
8	61	2160	7.2	73	20 ± 2	28 ± 1
6	61.4	2220	10.9	86	35 ± 4	34 ± 1

7a and 7b) with the same microstructure as previously observed in section 3.2 (Fig. 5). Some isolated crystals with a diameter in the range 2-15 µm were also identified (Fig. 7c). Some EDX local analysis, notably on the crystals and on the agglomerates, allowed to confirm that only Mg and O were present with a Mg content from 65 to 80 m%.

After 25 s, the measured temperatures were almost stable with a decrease of 1-2% on 620 s (Fig. 8a). An intense peak of CO around 25 s after the beginning of the recorded data characterized this carbothermal reduction (Fig. 8b). When the temperature increases from 2070 to 2200 K, the peak of the CO emitted also increases, which indicates that reaction kinetics are strongly improved with little temperature change in the studied range.

It had been observed that 100 s after the beginning, 50%, 67%, 80% and 80% of the total CO produced (measured after 620 s of reaction) were emitted respectively at 2070, 2140, 2160 and 2220 K. After the peak at maximum, the CO concentration decreases gradually to reach concentration lower than 400 ppm at 100 s. A slight peak of CO_2 was also recorded at the beginning of the experiment. Nevertheless, the maximum of this peak is lower than 500 ppm and the CO_2 partial pressure (< 0.5 Pa) is at least 10 times lower than the CO one (< 6 Pa). The production of CO_2 could result from the burning of the biochar impurities and also from a possible weak reaction between MgO and CO (Eq. 2) in the porous media while the CO production is higher at the beginning of the experiments.

It also appeared that the lower Mg content obtained in the powders collected from these experiments (compared to those of section 3.2) was due to the huge rise of the temperature at the beginning of the experiment, that produced a greater amount of CO and CO_2 favoring the reversion reaction of Eq. 1 and the oxidation of the condensed Mg by CO_2.

3.3.2. Kinetics calculations

Kinetics calculations were carried out to determine the main mechanisms of the carbothermal reduction of MgO. The reaction extent y used in these calculations is represented by:

$$y = x_c / x_i = n(CO)_t * (M(C)+M(MgO)) / x_i \quad (6)$$

where x_c is the consumed mass of reactants during experiments and x_i is the initial mass of the sample.

The three main mechanisms controlling a solid-state reaction, notably summarized by Sundar Murti and Seshadri [32], Ray [33] and Wang et al. [34] (kinetics studies on the carbothermal reduction of synthetic chromite but these general mechanisms are similar in the carbothermal reduction of other oxides

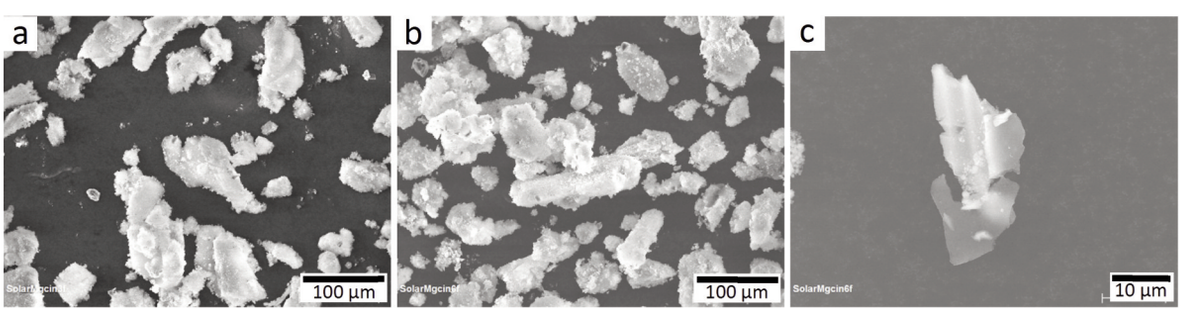

***Figure 7**. SEM images of the collected powder on the filter after experiments a) 3, b) and c) 6*

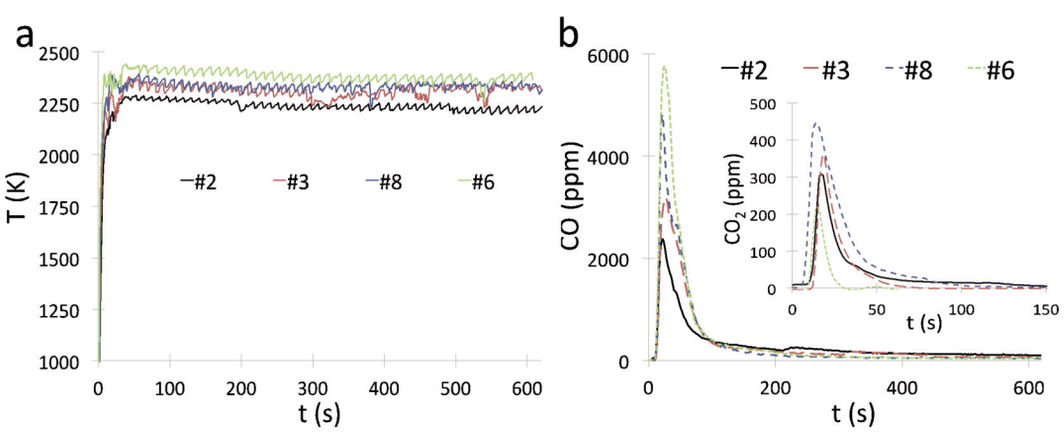

***Figure 8**. a) Temperature and b) Emitted CO and CO_2 (inserted graph) as a function of time for experiments 2, 3, 6 and 8*

like MgO), are:

- the phase boundary reaction, which is described by the Jander's equation linking the reaction extent with time (assuming spherical particles):

$$A = 1 - (1-y)^{1/3} = kt \quad (7)$$

- the diffusion of the reactant through a porous layer, which is described by the following relation:

$$B = 1 - (2/3)y - (1-y)^{2/3} = kt \quad (8)$$

- the nucleation of the product at active sites, which is represented by the relation (following the assumption that there is an equal probability of nucleation at each active site):

$$C = \ln(1/(1-y)) = kt \quad (9)$$

Considering only the CO emission to perform these calculations (Eq. 6), it was assumed that equimolar quantities of Mg and CO were produced at the same time and that the CO emitted corresponds to the Mg particles condensed on the filter (case with no reversion reaction).

Assuming isothermal conditions 15 s after the beginning of the experiment (duration of the shutter opening is around 10 s and the stabilization of the temperature is very fast on the surface of the pellet in concentrated solar processes), A, B and C expressions respectively issued from relations (7), (8) and (9) are represented versus time for experiment 6 in Figure 9a. It appeared that no simple kinetic relation was appropriate to describe an experiment on 620 s, i.e. several kinetic processes are involved in the carbothermal reduction of MgO. Three different kinetic stages were determined:

- during the first 20 s after the beginning of the experiment (16-36 s, stage I), an important emission of CO occurs (Fig. 8b) and the reaction rate is very high,
- the reaction rate decreases until 80 s (stage II) that corresponds to a huge decrease of the CO emission,
- the reaction rate is low and decreases very slowly (stage III).

Concerning the first step of the carbothermal reduction of MgO, the recorded data of the CO emission from 10 s before to 10 s after the maximum of CO emission obtained from experiments presented in section 3.3.1 (Fig. 8b) show a good correlation with relations (7) and (9), that respectively correspond to the phase boundary reaction and to the nucleation process (Fig. 9b). The diffusion phenomenon presents a poor correlation with the same data and thus it is not a dominant process at the beginning of the reaction. The activation energy of the processes at the initial stage of the reaction was calculated using the Arrhenius equation (Table 3):

$$k = A' \exp(-Ea/RT) \quad (10)$$

where A' is the pre-exponential factor, Ea the activation energy (kJ mol^{-1}), R the ideal gas constant (8.3145 J mol^{-1} K^{-1}) and T the temperature (K). Considering the temperature of the surface sample measured by optical pyrometry, the calculated activation energies are around 260-270 kJ mol^{-1} for the two dominant processes (phase boundary reaction

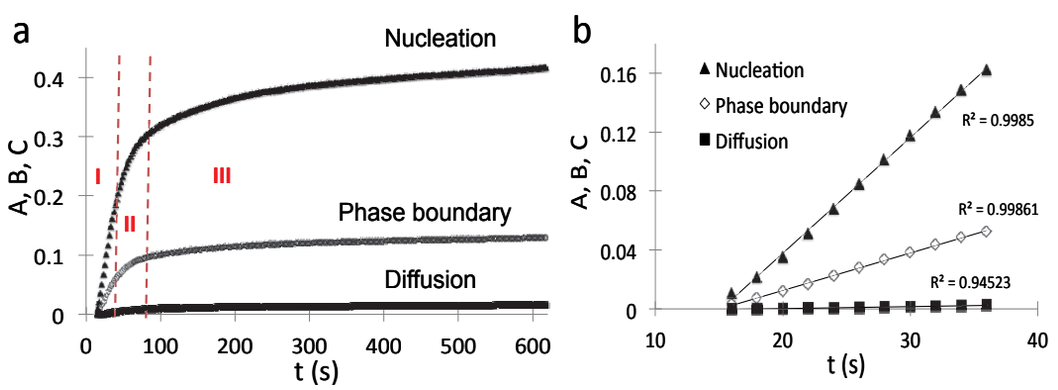

***Figure 9**. A, B and C expressions versus time a) for the whole duration of experiment 6, b) At the initial stage of experiment 6 (10 s before to 10 s after the CO maximum emission)*

***Table 3.** Activation energy (Ea) of the three mentioned reaction processes*

Reaction process	Ordinate kinetic law	Ea (kJ mol^{-1}) calculated at T_{pyro}*	Ea (kJ mol^{-1}) calculated at T_{pyro}*- 200 K
Phase boundary	$1-(1-y)^{1/3}$	260 ± 50	210 ± 50
Diffusion	$1-(2/3)y-(1-y)^{2/3}$	530 ± 100	440 ± 100
Nucleation	Ln(1/1-y)	270 ± 50	220 ± 50

and nucleation) of the first step whereas the one calculated for the diffusion process is twice (530 kJ mol^{-1}) with a lower correlation coefficient (Table 3). If it is considered that the temperature of the sample surface is overestimated of around 200 K, as it has been previously observed in first modeling results, the activation energy of the 3 processes are lowered by nearly 20%.

In the second stage, the best correlation corresponds to a phase boundary mechanism whereas in the third step, the three processes have almost similar correlation coefficients. In these two stages, the recirculation of gases in the reactor is important (low amount of gaseous CO/Mg diluted in Ar) and it is possible that several mechanisms are involved at the same time, which could not be described by simple kinetics relations as for the first stage.

4. Discussion

4.1. Analysis of the reaction products and residues

The microstructure of the collected powders observed after the carbothermal reduction of MgO allowed to obtain agglomerates of nanostructured Mg/MgO powders with a higher Mg content (90-98 m%) than those previously obtained [15] mainly due to a better tightness of the reactor (checked by an O_2 analyzer; i.e., in the present study the reversion is only caused by CO/CO_2). Some Mg crystals with a diameter in the range 2-15 µm were also identified in the present case. The great specific surface of these powders can be an advantage for future applications as solid fuels in combustion processes [8]. Total metallic yields close to 50 m% are promising and comparable to another recent solar process (with a cavity) used to reduce MgO with carbon in vacuum [16].

Some improvements were obtained using the biochar instead of the carbon black as reducing agent due to the fact that some impurities present in the biochar could catalyzed the reaction and that the morphology and the particle size of the biochar allowed a better homogeneity during the mixing with MgO particles. However, the Mg content in the collected powders after the experiments using biochar is also lower than with black carbon certainly due to the presence of more impurities in the biochar (emission of O_2, CO_2…).

It appeared that the residues on the sample-holder were porous (Fig. 6). Using the Scherrer equation, it had been calculated that the length of a cube edge of a crystallite from the reactant MgO (Periclase form) is equal to 13±4 nm whereas for a crystallite issued from MgO contained in the residue (experiments 33 and 35), the same parameter is equal to 74±10 nm, which indicated that MgO crystals had grown by a factor of 5-6 during the carbothermal reduction of MgO. The sintering of MgO grains at high temperature was previously observed or suggested [15, 16]. This phenomenon is supposed to be a reaction inhibitor because it diminishes the surface contacts between MgO and C grains. However, the presence of large grains of MgO (20-44 µm) is also a problem that had been already revealed [16]. So, the use of smaller grains of MgO could be useful to obtain higher yields.

4.2. Correlations between thermodynamics, reaction mechanisms and kinetics

The first vapors of gaseous Mg/CO appeared at measured temperature of 1500-1600 K, which is close to the thermodynamic calculations already realized at 900-1000 Pa for Eq. (1). On the other hand, the total Mg yield increased when the hold temperature was increased up to 2200 K (Table 3), which is more than 500 K higher than predicted by thermodynamics at 900-1000 Pa for a complete conversion of Eq. (1). The differences between the experimental observations and the preliminary modeling results implied a significant deviation between measured and real temperatures. This deviation has been evaluated close to 200 K but needs to be further clarified by future relevant studies with a realistic complete numerical model and other experimental configurations/device. Assuming this deviation, the carbothermal reduction of MgO could be realized at temperature close or lower than 2000 K, which is 300 K higher than predicted by thermodynamics at 900-1000 Pa for a complete conversion of Eq. (1). These high temperatures are required certainly because the magnesium is easily oxidized by residual CO_2 (CO_2 is less formed at high temperature considering Eq.(3)) and the contacts between MgO and C could certainly be better optimized.

In this study, temperatures between 1600 and 2220 K were reached in less than 15 s (100 - 150 $K.s^{-1}$). The intense CO peak produced at a hold temperature showed that the reaction is instantaneous and could be well described by a solid reaction between MgO and C grains at the initial stage of the experiments. Considering that the temperature on the sample surface is T_{pyro^*} minus 200 K, the calculated activation energy (Table 3) of the phase boundary reaction was close to those already calculated by other authors [16, 18]. The nucleation process presents a good correlation with the experimental data, close to the phase boundary reaction one (Fig. 9b) and the activation energy of the two processes are similar due to the fact that the data used correspond to CO emissions. However, these emissions could be different from the formed

condensed Mg during the whole experiments. So, further investigations in semi-continuous or continuous process are needed to better evaluate the kinetics of the carbothermal reduction of MgO on longer times and particularly to determine the nucleation rate of Mg.

After the first stage of the carbothermal reduction of MgO, the CO emissions quickly decreased (Fig. 8b) due to an important decrease of the surface reaction. The diffusion of the gaseous compounds inside the reactor could participate to the reaction but the activation energy of this process is very high compared to those of the phase boundary and the nucleation (Table 3). Furthermore, Chubukov et al. have recently demonstrated that solid-gas reaction are promoted only when the system pressure is higher, close to 10^4 Pa [22]. So, the reaction of Eq. (2) is not favored in the present study with a lower pressure close to 10^3 Pa.

Supplementary work will be performed in order to accurately evaluate the diffusion phenomenon and the nucleation rate of Mg in the two last stages of the experiments.

Concerning the experiments with a gradual increase of temperature (section 3.2), the metallic yields obtained at the end of the experiments were higher because this gradual increase during the whole experiments allowed activating again the phase boundary reaction in the depth of the sample (new CO peaks were produced when the temperature increased). So, gradual increases of the temperature, from 1000-1100 K in order to avoid the production of CO_2 from Eq. (3), are preferable to obtain higher yield in the solar carbothermal reduction of MgO. Considering T_{pyro} minus 200 K (Table 2), the maximum temperature reached in experiments 32 and 33 was close to 2000 K. The high Mg content obtained in these two experiments with adequate physico-chemical parameters and heat treatment proved that the reversion reaction during the experiments and the oxidation during the collection are weak. This is mainly due to low partial pressure of CO and CO_2 during the whole duration of the experiments (< 10 Pa and < 1 Pa respectively for PCO and PCO_2) [27]. Using an improved collection process of the powders (collection on all the metallic sections, better system to filter the particles…), higher metallic yields close to 65-70 m% could be obtained. Nevertheless, the main problem in the solar carbothermal reduction of MgO remains the presence of 20-30 m% of residue on the sample holder at the end of the experiment, which could be solved by developing a continuous process (as an example, with a fluidized bed reactor) and/or by using smaller MgO grains in future investigations.

5. Conclusion

The carbothermal reduction of MgO using concentrated solar energy was studied with the optimized reactor Sol@rmet that allows to measure in-situ temperature and CO/CO_2 emission during experiments. The collected powders are constituted by agglomerates of nanostructured grains and by some Mg crystals with a diameter in the range 2-15 µm. A maximum Mg content in the collected powders of 98 m% and a maximum yield of 50% were reached. Biochar as reducing agent appeared to produce better or similar results than carbon black certainly due to the presence of some more impurities in biochar. The dominant process identified at the initial stage of the reaction was attributed to a phase boundary reaction between MgO and C. Considering the measured temperature on the whole sample surface by optical pyrometry, the activation energy of this process is around 260 ± 50 kJ mol^{-1}. However, this measured temperature could be overestimated of around 200 K – taking into account our preliminary modeling results – that could decrease the activation energy to 210 ± 50 kJ mol^{-1}, closer to some values already calculated in the literature. The activation energy of the diffusion process is very high compared to the others and this process did not participate to the initial stage of the reaction. Future investigations will be done in order to accurately evaluate the nucleation rate of Mg and the diffusion phenomenon in the last stages. Low reversion reaction was obtained in several experiments with adequate physico-chemical parameters (low P_{CO} and P_{CO2}) and heat treatment but the main problem concerns the presence of an important residue at the end of reaction, which could be solved by developing a continuous process and by modifying some physico-chemical parameters of the reactants.

Acknowledgements

This work was supported by the PSA Peugeot-Citroën group and by the Programme "Investissements d'Avenir" (Investment for the Future) of the Agence Nationale de la Recherche (National Agency for Research) of the French State under award number ANR-10-LABX-22-01-SOLSTICE. The authors thank R. Masse for the thermal modeling results and O. Prévost for the realization of the solar reactor.

References

[1] R. Palumbo, A. Rouanet, G. Pichelin, Energy 20 (1995) 857-868.

[2] J. Millar, R. Palumbo, A. Rouanet, G. Pichelin, Energy 22 (1997) 301-309.

[3] A. Steinfeld, C. Larson, R. Palumbo, M. Foley, Energy 21 (1996) 205-222.

[4] R. Palumbo, J. Lédé, O. Boutin, E. Elorza Ricart, A. Steinfeld, S. Möller, A. Weidenkaff, E.A. Fletcher, J. Bielicki, Chem. Eng. Sci. 53(14) (1998) 2503-2517.

[5] A. Steinfeld, Energy 22 (1997) 311-316.

[6] A. Steinfeld, P. Kuhn, A. Reller, R. Palumbo, J. Murray, Y. Tamaura, Int. J. Hydrog. Energy 23 (1998) 767-774.

[7] M. Epstein, G. Olalde, S. Santén, A. Steinfeld, C. Wieckert, J. Solar Energy Eng. 130(1) (2008) 014505-014505-4.

[8] J.M. Bergthorson, S. Goroshin, M.J. Soo, P. Julien, J. Palecka, D.L. Frost, D.J. Jarvis, Appl. Energy 160 (2015) 368-382.

[9] R. Lomba, S. Bernard, F. Halter, C. Chauveau, C. Mounaïm-Rousselle, P. Gillard, T. Tahtouh, O. Guézet, Proc. 53rd AIAA Aerospace Sciences Meeting – AIAA Scitech, , Kissimmee, USA, 5-9th January 2015, p. 6986-7000.

[10] F.J. Hansgirg, Iron Age, Vol. 18, 1943, p. 56-63.

[11] H. Li, W. Zhang, Q. Li, B. Chen, Resources, Conservation and Recycling 100 (2015) 41–48.

[12] G. Feng, Z. Nie, Z. Wang, X. Gong, T.A. Zuo, Mater. Sci. Forum 685 (2011) 152-160.

[13] M.W. Jr Chase, NIST-JANAF, Thermochemical tables, 4th edition, J. Phys. Chem. Ref. Data, Monograph n°9, 1998.

[14] M. Halmann, A. Frei, A. Steinfeld, Min. Proc. Extract. Metall. Rev. 32 (2011) 247-266.

[15] J. Puig, M. Balat-Pichelin, J. Magn. Alloys 4 (2016) 140-150.

[16] I. Vishnevetsky, M. Epstein, Solar Energy 111 (2015) 236-251.

[17] L.H. Prentice, M.W. Nagle, Proc. Magnesium Technology 2009 (TMS), San Francisco, CA, United States, 2009, p. 35-39.

[18] M.E. Galvez, A. Frei, G. Albisetti, G. Lunardi, A. Steinfeld, Int. J. Hydrog. Energy 33 (2008) 2880-2890.

[19] L. Rongti, W. Pan, S. Masamichi, Metall. Mater. Trans. B 34 (2003) 433-437.

[20] W.D. Xie, J. Chen, H. Wang, X. Zhang, X.D. Peng, Y. Yang, Rare Metals 35(2) (2016) 192-197.

[21] R.J. Fruehan, L.J. Martonik, Metall. Mater. Trans. B 7 (1976) 537-542.

[22] B.A. Chubukov, A.W. Palumbo, S.C. Rowe, I. Hischier, A.J. Groehn, Thermochimica Acta 636 (2016) 23-32.

[23] E.Y. Shafirovich, U.I. Goldshleger, Combustion Sci. Tech. 84 (1992) 33-43.

[24] G. Brooks, S. Trang, P. Witt, M.N.H. Khan, M. Nagle, JOM 58 (2006) 51-55.

[25] J. Engell, S. Frederiksen, K.A. Nielsen, US patent 5803947, 1998.

[26] L.H. Prentice, M.W. Nagle, T.R.D. Barton, S. Tassios, B.T. Kuan, P.J. Witt, K.K. Constanti-Carey, Proc. Magnesium Technology 2012 (TMS), Orlando, FL, United States, 2012, p. 31-35.

[27] I. Hischier, B.A. Chubukov, M.A. Wallace, R.P. Fisher, A.W. Palumbo, S.C. Rowe, A.J. Groehn, A.W. Weimer, Solar Energy 139 (2016) 389-397.

[28] Y.S. Touloukian, D.P. Dewitt, Thermophysical properties of matter - Thermal radiative properties - Non metallic solids, Vol. 8, Plenum: New-York, 1972.

[29] F.H. Chung, J. Appl. Cryst. 7 (1974) 519-525.

[30] R.L. Snyder, Powder Diffr. 7 (1992) 186-193.

[31] E. Ya. Shafirovich and U.I. Goldshleger, Combustion Science and Technology 84 (1992), 33-43.

[32] N.S. Sundar Murti, V. Seshadri, Transact. Iron Steel Instit. Japan 22(12) (1982) 925-933.

[33] H. Ray, Kinetics of metallurgical reactions, Oxford and IBH Publishing: New Delhi, 1993.

[34] Y. Wang, L. Wang, J. Yu, K.C. Chou, J. Min. Metall. Sect. B-Metall. 50(1) B (2014) 15-21.

EKSPERIMENTALNO ISPITIVANJE KARBOTERMIČKE REDUKCIJE MGO NA NISKOM PRITISKU UZ KORIŠĆENJE KONCENTROVANE SOLARNE ENERGIJE

J. Puig *, M. Balat-Pichelin

PROMES-CNRS laboratorija, Font-Romeu Odeillo, Francuska

Apstrakt

Usavršeni solarni reaktor Sol@rmet omogućava da se istraži redukcija MgO u prisustvu ugljenika korišćenjem koncentrovane solarne energije u uslovima niskog vakuuma, oko 900 Pa. Analiziran je uticaj vrste ugljenika, i pokazalo se da je ugljenik iz biomase odličan kandidat. Postepeno povećanje temperature tokom eksperimenta omogućilo je dobijanje obećavajućih rezultata. Dobijeni su prahovi sa visokim sadržajem Mg do 97 m%, i sa visokim prinosom do 50 %. Izvršeni su kratkotrajni eksperimenti na određenim lokacijama u žarištu solarnog koncentratora da bi se dobile informacije o kinetici karbotermičke redukcije MgO. Sprovedeni eksperimenti su istakli uticaj temperature na CO emisiju. 50 do 80% emisije CO uglavnom se dešava u prvih 100 sekundi od početka eksperimenta. Utvrđeno je da je reakcija na međugraničnoj površini MgO i C dominantan proces u inicijalnoj fazi karbotermičke redukcije. Izračunata energija aktivacije ovog procesa je oko 260 kJ mol^{-1}.

Ključne reči: *Karbotermička redukcija; Koncentrovana solarna energija; XRD karakterizacija; Mikrostruktura; Kinetika*